

Chapter 5

ATM VP-Based Ring Network Exclusive Video or Data Traffics

In this chapter, the performance characteristic of the proposed ATM VP-Based Ring Network exclusive video or data traffic is studied. The maximum capacity is also located for unidirectional and bi-directional nodes, however, the results indicate that the capacity is double in case of using unidirectional nodes. We have to mention here that some of performance results are closed to the results in [51], such as the relation between the offered loads versus end-station delays, inspite the difference in the proposed model and generation of traffic.

We have explained the relationship between number of video sources (N_{vi}) and many parameters such as Mean Waiting Time (MWT) which represents the time spent in the queue from the last bit arrived to the whole cell delivered, and Maximum Buffer Size (MBS) required for supporting the sources. The following represents the definition we have used such as the Utilization of the node as (U), the Throughput as (TP), the fixed video encoding rate as (R_{vi}), and the Offered video Load as (OL_{vi}). The frame transmission time (t_f) is 0.125 ms depending on SONET STS-3c, the frame size (F_s) is 44 cells depending on both cell size (53 octets) and payload size in transmission frame (2340 octets). However, the calculation of the transmission rate (R_T) is given by the following equation (5-1).

$$R_T = \frac{F_s(\text{cells})}{t_f(\text{ms})} = 352 \text{ cell/ms} \quad \dots\dots\dots (5-1)$$

..

The transmission rate ($R_T = 352 \text{ cell/ms}$) is used for the supported video sources and the transit cells (i.e. the cells coming from previous node to next node). The transit rate has the range from 0 cell/ms to 352 cell/ms, and the

average transit rate (GR_t) theoretically is calculated from the following equation (5-2).

$$GR_t = \frac{352(\text{cell/ms}) - 0(\text{cell/ms})}{2} = 176 \text{ cell/ms} \quad \dots\dots\dots (5-2)$$

5-1 ATM Exclusive Video Traffic Only.

Video traffic is represented as video stream and generated from codec for various encoding rates such as MPEG (2 and 1.5 Mbps), H.261 (384 Kbps), and low quality (192 Kbps), as explained in chapter 3.

The main goal is to locate the maximum capacity of the video sources (N_{vi}), which depends on R_{vi} . However, the ideal maximum values of N_{vi} depends on R_{vi} (Kbps) and $R_T = 352 \text{ cell/ms}$, follows the SONET physical transmission as can seen in the following equations (5-3) and (5-4)

$$\text{max. } N_{vi} = \frac{352(\text{cell/ms}) - \text{transit_rate}(\text{cell/ms})}{GR_{vi}(\text{cell/ms})}, \quad \dots\dots\dots (5-3)$$

$$\text{where, } GR_{vi} = \frac{R_{vi}(\text{Kbps})}{47(\text{octets}) \times 8(\text{bits})} (\text{cell/ms}) \quad \dots\dots\dots (5-4)$$

Using equations (5-3) and (5-4) helps to calculate GR_{vi} , for each video source and maximum N_{vi} for various values of R_{vi} . Table 5-1 summaries the ideal maximum N_{vi} for various values of R_{vi} .

From Table 5-1, obviously the increasing of R_{vi} decreases N_{vi} , this is because the increasing of R_{vi} increases GR_{vi} (from equation 5-4); resulting in increases number of video cells generated, which has significant effect on the number of video sources (N_{vi}) that can be served by the network.

In fact the measured N_i definitely would be less or equal to that ideal calculated values.

R_{vi}	Ideal max. N_{vi}
192 Kbps	345
384 Kbps	173
1.5 Mbps	44
2.0 Mbps	34

Table 5-1 Ideal Maximum N_{vi}

The following values of R_{vi} we have used in our simulation studies: 192 Kbps, 384 Kbps, 1.5 Mbps, and 2 Mbps respectively. That is to study the video MWT, MBS, U_{vi} , and TP_{vi} versus N_{vi} , and video MWT and MBS versus offered load (OL_{vi}).

Figure 5-1 shows video MWT versus N_{vi} sources, for the values of R_{vi} have mentioned above. From Figure 5-1 obviously that the increasing of R_{vi} , increases number of cells resulting in decreases the number of video sources (N_{vi}). The video MWT slightly increases with the increasing of N_{vi} up to the saturation limits after that video MWT sharply increases due to the large number of cells and queuing delay. It is to be mentioning here that the saturation limit that corresponds to the maximum N_{vi} decreases with the increasing of R_{vi} according to the equations 5-3, and 5-4.

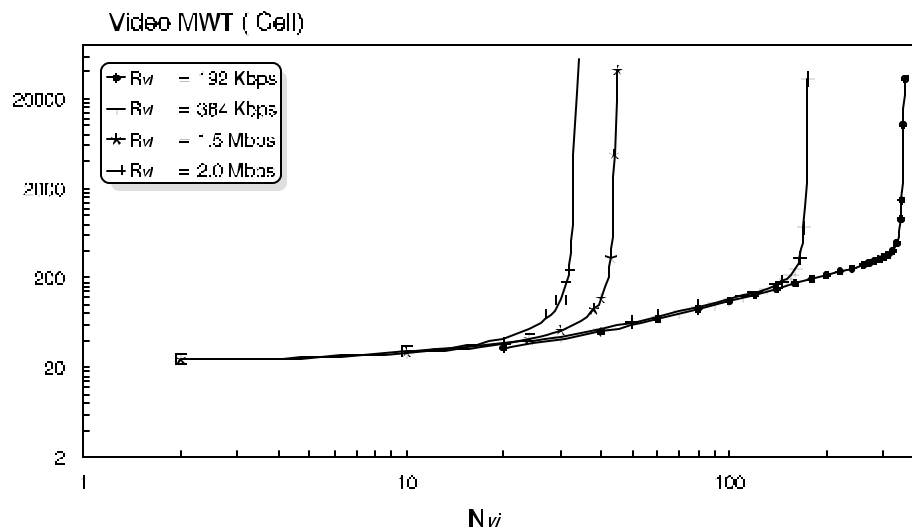
Figure 5-1 Video MWT versus N_{vi} .

Figure 5-2 depicts video MWT versus OL_{vi} . The video MWT slightly increases with the increasing of OL_{vi} up to the saturation limit then video MWT sharply increases due to the fact that the generated video cells are much more than the transmitted cells resulting in long video MWT. The video MWT decreases as R_{vi} increases because the transmission of cells increases with the high R_{vi} resulting in short video MWT.

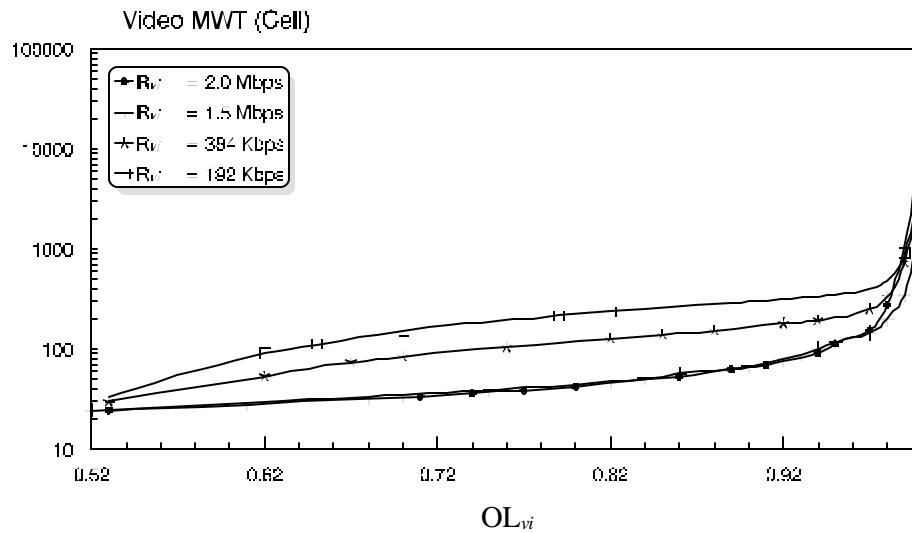


Figure 5-2 Video MWT versus OL_{vi} .

Figure 5-3 illustrates video MBS in cells versus N_{vi} , for the values of R_{vi} mentioned above. The video MBS is the maximum number of cells enters to input video queue at any time. It may be less than the maximum value, and not more. The behavior is similar to that of Figure 5-1. So, the video MBS slightly increases with the increasing of N_{vi} up to the saturation limit, after that the video MBS sharply increases, this is due to the large number of cells waiting in the queue for transmission. The video MBS and N_{vi} decrease as the R_{vi} increases for the same reasons mentioned with Figure 5-1.

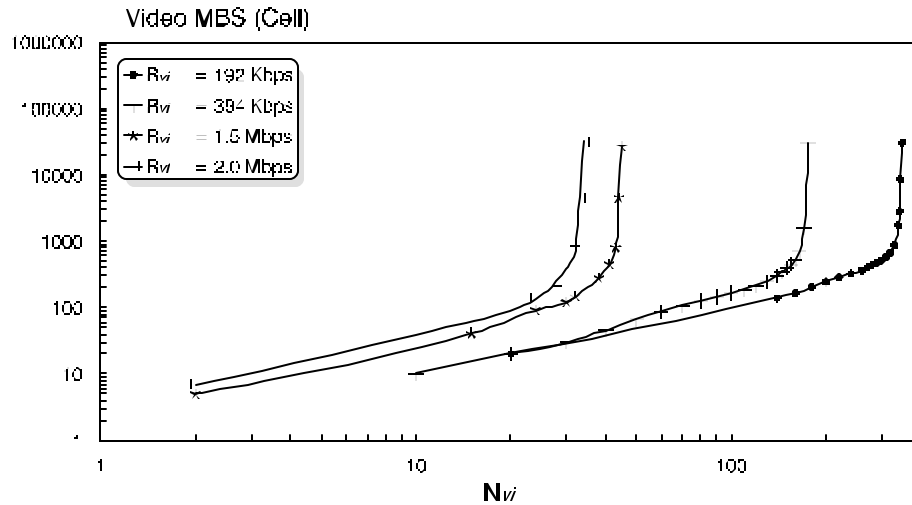
Figure 5-3 Video MBS versus N_{vi} .

Figure 5-4 depicts video MBS versus OL_{vi} . The video MBS slightly increases with the increasing of OL_{vi} up to the saturation limit then video MBS sharply increases due to the fact that the generated cells are much more than the transmitted cells resulting in large number of video cells waiting for transmission (i.e. large video MBS). The video MBS decreases as R_{vi} increases because the transmission of cells increases with the high R_{vi} resulting in small video MBS (similar to Figure 5-2).

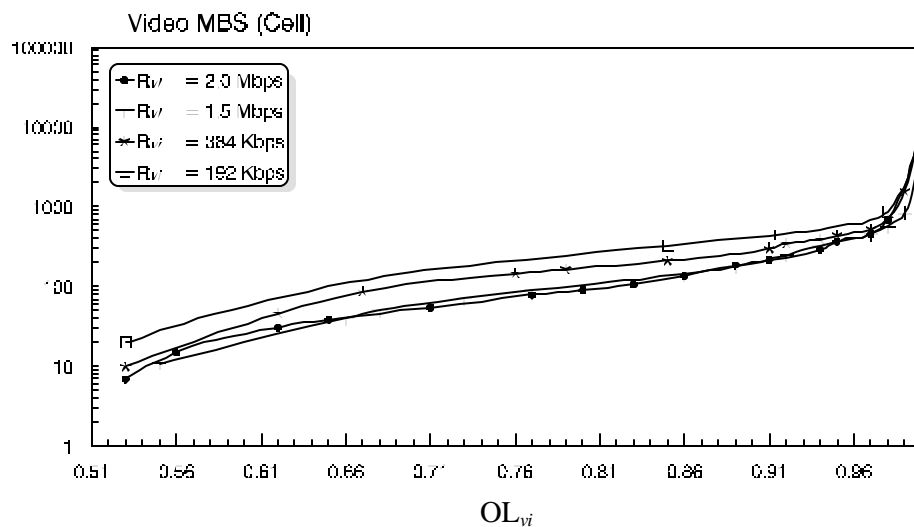
Figure 5-4 Video MBS versus OL_{vi}

Figure 5-5 shows U_{vi} versus N_{vi} . The U_{vi} remains constant with the increasing of N_{vi} , up to the saturation limit of N_{vi} , then U_{vi} slightly decreases, this is because after the saturation limit the node couldn't serve any video cells resulting in decreases of U_{vi} . It is to be mention here. That the saturation limit depends upon R_{vi} that is because the number of the generated cells is almost equal to the service duration of these generated number of cells, resulting in constant value of U_{vi} .

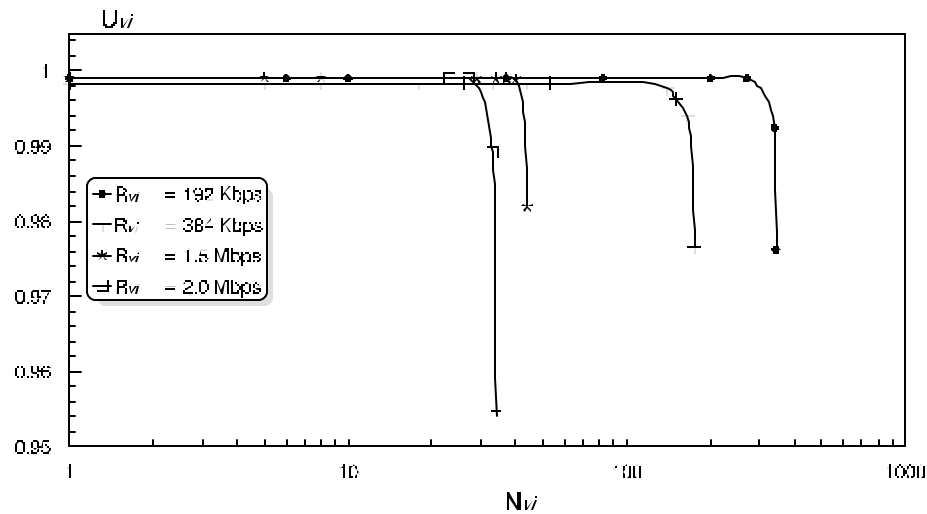


Figure 5-5 U_{vi} versus N_{vi}

Figure 5-6 illustrates TP_{vi} versus N_{vi} . From the Figure the increasing of N_{vi} , increases TP_{vi} up to saturation limits. Beyond the saturation limits, the TP_{vi} remains constant because the generated number of video cells is greater than the number of cells to be served. Also, it is clear that the increasing of R_{vi} , reduces N_{vi} (i.e. reduces the saturation limits). Table 5-2 summaries the results of the proposed ATM/ADM exclusively video traffic only.

R_{vi}	N_{vi}	Video MWT (cell)	Video MBS (cell)	OL_{vi} (ratio)	U_{vi} (ratio)
192 Kbps	342	1490.7	2819	0.997	0.993
384 Kbps	170	732.14	1579	0.994	0.994
1.5 Mbps	43	346.96	827	0.988	0.999
2.0 Mbps	32	277.6	700	0.984	0.999

Table 5-2.

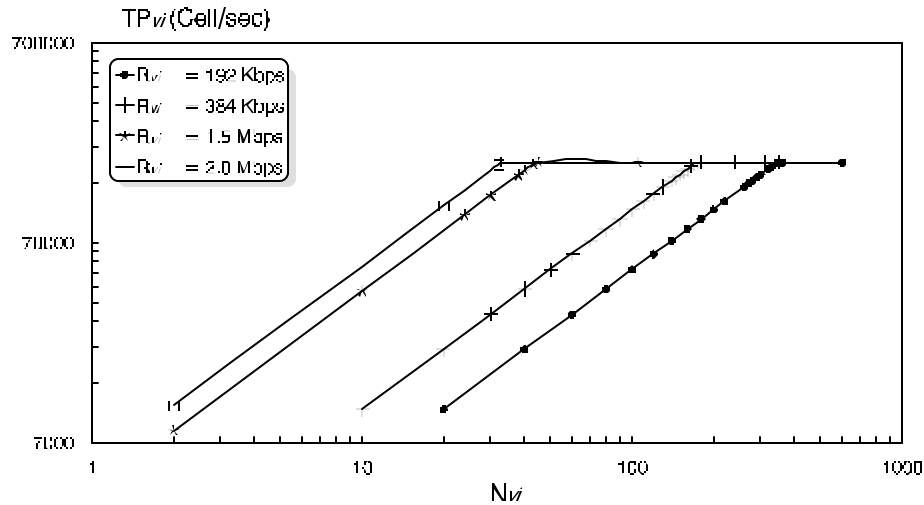


Figure 5-6 TP_{vj} versus N_{vj} .

5-2 ATM Exclusive Data traffic only

The data traffic consists of one message or several messages, its arrival process defined by two parameters; message size (M_{siz}) and interarrival time which is presented by an exponential distribution with mean values (μ) equal to 5 and 10 ms, as explained in chapter 3.

The ideal maximum message size (M_{siz}) which depends on μ can be calculated from the following equations (5-5) and (5-6).

$$\max. M_{siz} = \frac{352(\text{cell / ms}) - \text{transit_rate}(\text{cell / ms})}{(1 / m)\text{cell / ms}}, \dots\dots\dots (5-5)$$

$$\text{where, } GR_{da} = \frac{M_{siz}(\text{Cell})}{m}(\text{cell / ms}) \dots\dots\dots (5-6)$$

By substituting in the above equations (5-5) and (5-6), we can get the ideal maximum M_{siz} for various values of μ , obviously from the equations the increasing of μ , increases M_{siz} . Table 5-3 summaries the ideal maximum M_{siz} will full load carried by the node (i.e. OL_{da} 100 %)

μ	Ideal max. M_{siz}
5 ms	880
10 ms	1760

Table 5-3 the Ideal max. M_{siz} cells.

In our simulation studies, we have assumed that μ equals to 5 and 10 ms respectively, that is to study the different performance characteristics such as data MWT, MBS, U_{da} , and TP_{da} versus M_{siz} , data MWT and MBS versus OL_{da} .

Figure 5-7 depicts Data MWT versus M_{siz} . The data MWT smoothly increases with the increasing of M_{siz} up to certain M_{siz} (depending on the value of μ). The data MWT increases more than started values of M_{siz} , this is because the increases of M_{siz} increase the service times, resulting in long queue and the data message suffers long MWT. Within the interval 5 ms, the node transmits $\frac{\mu(ms)}{t_f(ms)} = \frac{5ms}{0.125ms} = 40$ frames, each frame includes an average of 22 cells. The M_{siz} of 500 cells needs to $(500\text{cells}/22\text{cell}/\text{frame})$ 23 frames. Then, the needed frames are less than the transmitted frames within 5 ms.

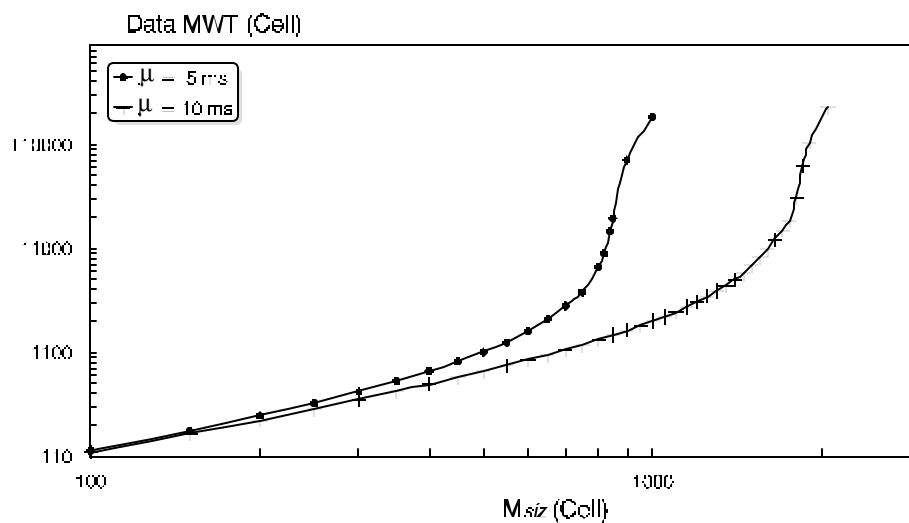
Figure 5-7 Data MWT versus M_{siz} .

Figure 5-8 shows data MWT versus OL_{da} . Clearly that the data MWT is slightly increases with the increasing of OL_{da} up to the saturation limit, then it sharply increases for the same reasons mentioned above. The absolute value of MWT depends upon the value of μ . Obviously, that the increasing of μ increases the MWT, this is because the increases of μ , increases the M_{siz} resulting in very long MWT.

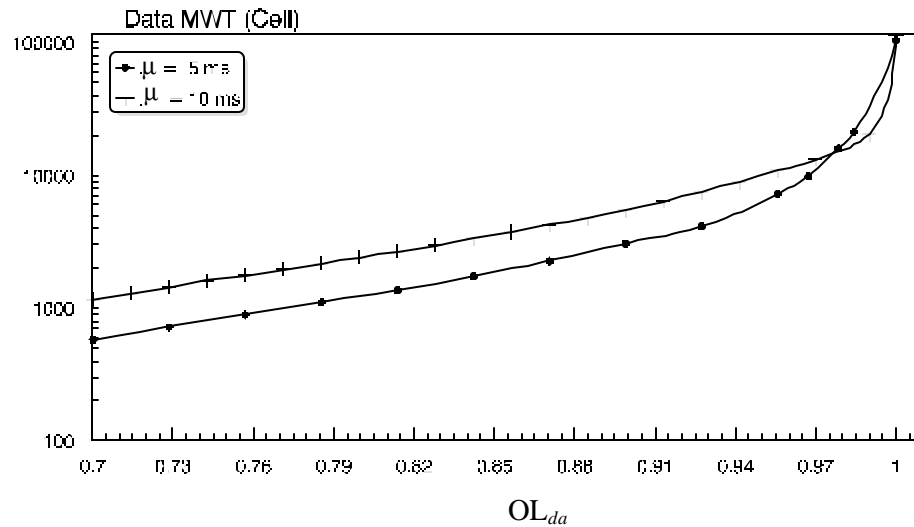


Figure 5-8 Data MWT versus OL_{da} .

Figure 5-9 illustrates data MBS versus M_{siz} . From the Figure, it is clear that the increasing of M_{siz} slightly increases data MBS up to saturation limits. Beyond the saturation limits, the data MBS is rapidly increase for the same reasons mentioned with Figures 5-7 and 5-8.

Figure 5-10 shows data MBS versus OL_{da} . The data MBS slightly increases with the increasing of OL_{da} up to the saturation limit, then data MBS sharply increases due to the same reasons mentioned above. It is to be mention here that the data MBS decreases as n decreases, because μ has a significant effect in M_{siz} , however, the decreasing of μ decreases M_{siz} resulting in short service time, which yields short queue and data MBS.

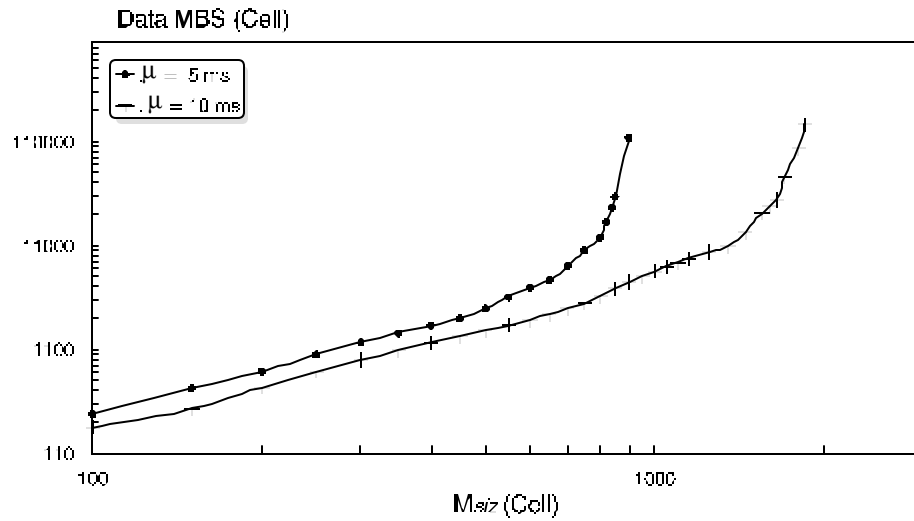
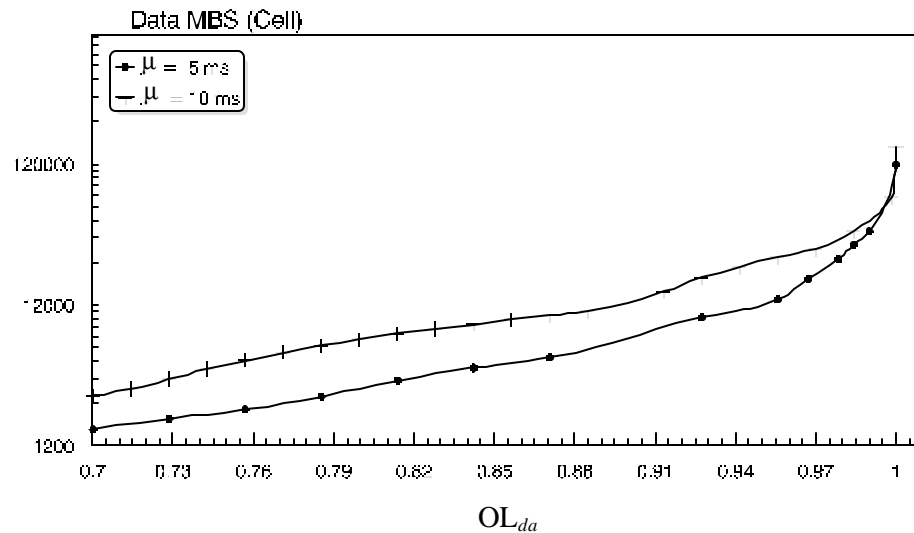
Figure 5-9 Data MBS versus M_{siz} .Figure 5-10 Data MBS versus OL_{da}

Figure 5-11 depicts U_{da} versus M_{siz} with μ equal to 5 and 10 ms respectively. The M_{siz} has no affect on U_{da} , therefore, U_{da} remains constant up to saturation limits which corresponding to the optimal M_{siz} , beyond U_{da} sharply decreases, because the increases of M_{siz} after optimal length decreases the

number of cells to be service resulting in decreases the U_{da} . Obviously, that with long μ the number of cells generated reduces, therefore, the saturation limit (optimal M_{siz}) is with longer M_{siz} as shown in Figure 5-11 ($\mu = 10$ ms). It is necessary to mention here that the optimal M_{siz} (saturation limit) depends upon μ , in which optimal M_{siz} increases with the increasing of μ .

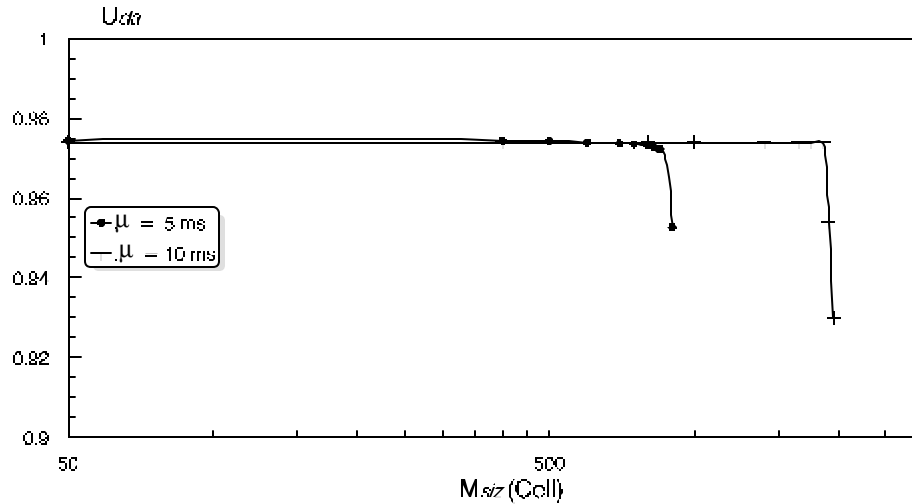
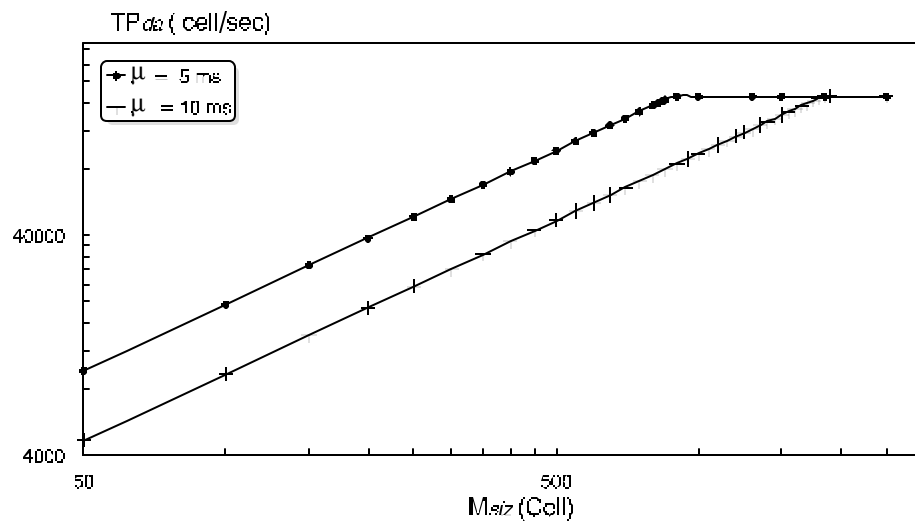


Figure 5-11 U_{da} versus M_{siz}

Figure 5-12 depicts TP_{da} versus M_{siz} . Obviously, that the increasing of M_{siz} , increases TP_{da} up to the saturation limits. Beyond the saturation limits, TP_{da} remains content because there is no chance for more service to cells. Again, recall that the saturation limit depends on μ . Table 5-4 summaries the results of the proposed ATM/ADM exclusively data traffic only.

μ	M_{siz}	Data MWT (cell)	Data MBS (cell)	OL_{da} (ratio)	U_{da} (ratio)
5 ms	860	28133.9	32580	0.997	0.99
10 ms	1750	20422.0	32652	0.998	0.99

Table 5-6

Figure 5-12 TP_{da} versus M_{siz}